

An Off-axis Jet Model for Multi-wavelength Afterglow Emission of GRB 190829A detected by H.E.S.S.

Yuri Sato,^{a,*} Kaori Obayashi,^a Ryo Yamazaki,^{a,b} Kohta Murase,^{c,d,e,f} Yutaka Ohira^g
and Shuta J. Tanaka^{a,h}

^aDepartment of Physical Sciences, Aoyama Gakuin University, 5-10-1 Fuchinobe, Sagamihara, Kanagawa 252-5258, Japan

^bInstitute of Laser Engineering, Osaka University, 2-6, Yamadaoka, Suita, Osaka 565-0871, Japan

^cDepartment of Physics, The Pennsylvania State University, University Park, Pennsylvania 16802, USA

^dDepartment of Astronomy and Astrophysics, The Pennsylvania State University, University Park, Pennsylvania 16802, USA

^eCenter for Multimessenger Astrophysics, Institute for Gravitation and the Cosmos, The Pennsylvania State University, University Park, Pennsylvania 16802, USA

^fCenter for Gravitational Physics and Quantum Information, Yukawa Institute for Theoretical Physics, Kyoto University, Kyoto, Kyoto 606-8502, Japan

^gDepartment of Earth and Planetary Science, The University of Tokyo, 7-3-1 Hongo, Bunkyo-ku, Tokyo 113-0033, Japan

^hGraduate School of Engineering, Osaka University, 2-1 Yamadaoka, Suita, Osaka 565-0871, Japan

E-mail: yuris@phys.aoyama.ac.jp

In the past three years, ground-based Imaging Atmospheric Cherenkov Telescopes, such as the Major Atmospheric Gamma Imaging Cherenkov (MAGIC) telescopes and the High Energy Stereoscopic System (H.E.S.S.), have reported the detection of the very-high-energy (VHE) gamma-ray photons from four gamma-ray bursts. One of them, GRB 190829A, was detected by H.E.S.S. with ~ 20 sigma significance. This event had more peculiar features. First, the prompt emission had much smaller isotropic equivalent gamma-ray energy than typical long gamma-ray bursts. Second, the early X-ray and optical light curves had achromatic peaks at 1.4×10^3 s. We propose an off-axis jet model to explain those unusual observed properties. In this model, the relativistic beaming effect causes the apparently small isotropic gamma-ray energy and spectral peak energy. We find that a narrow fast jet with the initial Lorentz factor of 350 and the initial jet opening half-angle of 0.015 rad, viewed off-axis, can describe the observed achromatic peaks in the X-ray and optical light curves. Another slow-wide jet explains the late X-ray and radio fluxes. Our model parameters determined by X-ray, optical and radio afterglows may explain observed VHE gamma-ray flux by synchrotron self-Compton (SSC).

7th Heidelberg International Symposium on High-Energy Gamma-Ray Astronomy (Gamma2022)
4-8 July 2022
Barcelona, Spain

*Speaker

1. Introduction

The ground-based Imaging Atmospheric Cherenkov Telescopes, such as the Major Atmospheric Gamma Imaging Cherenkov (MAGIC) telescopes and the High Energy Stereoscopic System (H.E.S.S.) reported the detection of the very-high-energy (VHE) gamma-ray photons from the GRBs 180720B [1], 190114C [2], 190829A [3] and 201216C [4]. GRB 190829A was classified as a low-luminosity GRBs [5]. The prompt emission of GRB 190829A had two episodes (Episode 1 and 2) [5]. The values of the isotropic gamma-ray energy $E_{\text{iso},\gamma}$ and the peak photon energy of the νF_ν spectrum, E_p , of both Episodes 1 ($E_{\text{iso},\gamma} = 3.2 \times 10^{49}$ erg and $E_p = 120.0$ keV) and 2 ($E_{\text{iso},\gamma} = 1.9 \times 10^{50}$ erg and $E_p = 10.9$ keV) were smaller than in typical long GRBs [5]. The multi-wavelength afterglows, in the VHE gamma-ray [3], X-ray, optical/infrared (IR) [5] and radio bands [8–10], of GRB 190829A were obtained. The X-ray and optical light curves had achromatic peaks at 1.4×10^3 s [5]. Several models were considered for the achromatic peaks, the X-ray flare model [5, 11], baryon loaded outflow model [12], e^+e^- dust shell model [13] and reverse-shock emission model [9, 10]. The VHE gamma-ray afterglow emission from GRB 190829A was detected by H.E.S.S. in the 0.2–4.0 TeV band at $t \sim 2 \times 10^4$ s after the burst onset [3]. For GRB 190829A, Salafia et al. [9] supposed the SSC emission viewed on-axis ($\theta_v \sim 0$), while Zhang et al. [11] proposed the external inverse-Compton emission.

In this proceeding, we consider an off-axis jet model in order to explain those unusual properties of GRB 190829A. In this model, if we see the jet in the off-axis ($\theta_v < \theta_j$) viewing, the prompt emission is dimmer and softer than on-axis ($\theta_v \sim 0$) viewing case due to the relativistic beaming effects [14, 15]. The bulk Lorentz factor is initially high, so that the afterglow emission is very dim because of the relativistic effect. When the jet decelerates, the beaming effect becomes weak. Then, a rising part emerges in afterglow light curves. For more details, see our papers (Sato et al. [16, 17]).

2. Model

Following Huang et al. [18], we calculate the dynamics of a relativistic jet [see 16, for details]. The jet has an isotropic-equivalent kinetic energy $E_{\text{iso,K}}$, initial jet Lorentz factor Γ_0 and initial jet opening half-angle θ_0 . It decelerates via the ambient interstellar matter (ISM) n_0 and forms a thin shell. We calculate the synchrotron radiation output assuming a power-law electron energy distribution with an index p and constant microphysics parameters ϵ_e , ϵ_B and f_e , which are the energy fractions of the internal energy going into power-law electrons and magnetic field, and the number fraction of accelerated electrons, respectively.

In calculating the VHE gamma-ray radiation, we assume the synchrotron self-Compton (SSC) emissions [19]. The Klein-Nishina effect affects the SSC flux [e.g. 11, 20–22], and it is considered. For the calculation of the extragalactic background light (EBL) absorption, Franceschini, Rodighiero, & Vaccari [23] is adopted and ‘EBL table’¹ is used. We get the flux density by integrating the emissivity over the equal arrival time surfaces (EATS) [see 24, for details].

¹<https://pypi.org/project/ebhtable/>

3. Results

In this section, we show our numerical results of afterglow light curves in the VHE gamma-ray (0.1 TeV), X-ray (5 keV), optical (V-band) and radio (1.3, 5.5, 15.5 and 99.8 GHz) bands, and compare them with the observation data of GRB 190829A. The VHE gamma-ray data are extracted from H.E.S.S. Collaboration et al. [3]. The X-ray data are downloaded from the *Swift* team website² [25, 26]. The optical data are taken from Chand et al. [5]. The V-band extinction is adopted as $A_V = 1.5$ mag [5]. The radio flux at 1.3 and 15.5 GHz and at 5.5 and 99.8 GHz bands are obtained from Rhodes et al. [8] and Dichiara et al. [10], respectively.

A single jet viewed off-axis is considered in order to explain the observed X-ray and optical achromatic peaks around $T \sim 1.4 \times 10^2$ s. We find the parameters, $\theta_v = 0.031$ rad, $\theta_0 = 0.015$ rad, $E_{\text{iso,K}} = 4.0 \times 10^{53}$ erg, $\Gamma_0 = 350$, $n_0 = 0.01$ cm⁻³, $p = 2.44$, $\epsilon_B = 6.0 \times 10^{-5}$, $\epsilon_e = 3.5 \times 10^{-2}$ and $f_e = 0.2$ to fit the data. In the following, we label this parameter space configuration as ‘narrow-jet’. The observational results of the early X-ray and optical afterglows from about 8×10^2 to 2×10^4 s are well explained by our off-axis afterglow model. The off-axis afterglow started with a rising part because of the relativistic beaming effect, which causes fewer photons emitted in the direction of an observer [27]. When the jet decelerates, the observed flux increases. If we assume the adiabatic evolution ($\Gamma \propto t^{-3/8}$), the observer time of the flux maximum is given by [16],

$$T_{\text{peak}} \sim (1+z) \left(\frac{3E_{\text{iso,K}}}{4\pi n_0 m_p c^5} \right)^{\frac{1}{3}} (\theta_v - \theta_0)^{\frac{8}{3}}. \quad (1)$$

For our narrow jet parameters, $T_{\text{peak}} \sim 2 \times 10^3$ s is obtained. It is consistent with our numerical results within a factor of two. However, our numerical results of the late X-ray and radio bands are dimmer than observed. Therefore, we assume that another wide jet component is arising at late times, following the model explained in Sato et al. [16, 17].

We introduce a ‘wide jet’ in addition to the narrow jet. The parameters of the wide jet are $\theta_v = 0.031$ rad, $\theta_0 = 0.1$ rad, $E_{\text{iso,K}} = 1.0 \times 10^{53}$ erg, $\Gamma_0 = 20$, $n_0 = 0.01$ cm⁻³, $p = 2.2$, $\epsilon_B = 1.0 \times 10^{-5}$, $\epsilon_e = 0.29$ and $f_e = 0.35$. It is assumed that both jets are uniform, and on co-axis, and they are emitted from the central engine at the same time. We compare the superposition of each jet emission with the observed light curve. One can find that our off-axis narrow jet emission explains the early achromatic peaks in the X-ray and optical bands (dashed lines in Fig. 1), and that the wide jet emission can explain the late X-ray and radio afterglows (dotted lines in Fig. 1). Our two-component jet model well explains the VHE gamma-ray flux.

4. Discussion

We have investigated an off-axis jet model to explain the observed data of GRB 190829A. According to our model, the early X-ray and optical light curves were off-axis emissions from the narrow jet, and the late X-ray and radio fluxes came from the wide jet emission. We found that the observed VHE gamma-ray emission of GRB 190829A could be explained by our off-axis two-component jet model.

²https://www.swift.ac.uk/xrt_curves/00922968/

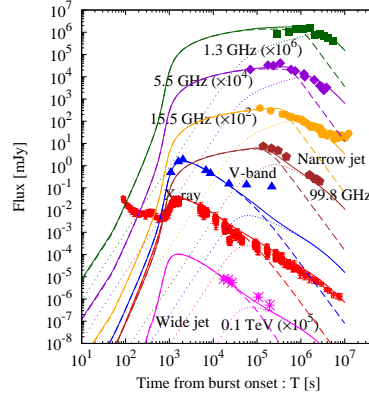


Figure 1: Afterglow light curves calculated by our two-component jet model – solid lines are the sum of the narrow jet (dashed lines: $\theta_v = 0.031$ rad, $\theta_0 = 0.015$ rad, $E_{\text{iso,K}} = 4.0 \times 10^{53}$ erg, $\Gamma_0 = 350$, $n_0 = 0.01$ cm $^{-3}$, $p = 2.44$, $\epsilon_B = 6.0 \times 10^{-5}$, $\epsilon_e = 3.5 \times 10^{-2}$, and $f_e = 0.2$) and the wide jet (dotted lines: $\theta_v = 0.031$ rad, $\theta_0 = 0.1$ rad, $E_{\text{iso,K}} = 1.0 \times 10^{53}$ erg, $\Gamma_0 = 20$, $n_0 = 0.01$ cm $^{-3}$, $p = 2.2$, $\epsilon_B = 1.0 \times 10^{-5}$, $\epsilon_e = 0.29$, and $f_e = 0.35$) in 0.1 TeV (magenta), X-ray (red), V-band (blue), 1.3 GHz (green), 5.5 GHz (violet), 5.5 GHz (orange) and 99.8 GHz (brown), which is compared with observed data of GRB 190829A (0.1 TeV (magenta points), X-ray (red points), V-band (blue triangles), 1.3 GHz (green squares), 5.5 GHz (violet diamonds), 15.5 GHz (orange filled-circles) and 99.8 GHz (brown pentagons).

The prompt emission of GRB 190829A had smaller values of the peak energy E_p and the isotropic-equivalent gamma-ray energy $E_{\text{iso},\gamma}$ than typical long GRBs. Here, we discuss whether E_p and $E_{\text{iso},\gamma}$ from our narrow jet were typical or not in the case of on-axis viewing ($\theta_v \approx 0$). A simple emission model is considered [14, 15, 28, 29]. We assume an instantaneous emission of an infinitesimally thin shell moving with the Lorentz factor Γ_0 . If Episode 1 of observed prompt emission was emitted from the narrow jet, that is, $E_p(\theta_v = 0.031) = 120$ keV and $E_{\text{iso},\gamma}(\theta_v = 0.031) = 3.2 \times 10^{49}$ erg [5], then we obtain on-axis quantities, $E_p(0) = 3.7$ MeV and $E_{\text{iso},\gamma}(0) = 2.7 \times 10^{53}$ erg (for details, see Sato et al. [16]). We calculate the efficiency of the prompt emission as $\eta_\gamma = E_{\text{iso},\gamma}(0)/(E_{\text{iso},\gamma}(0) + E_{\text{iso,K}}) \approx 0.4$. On the other hand, if the narrow jet emitted Episode 2 ($E_{\text{iso},\gamma}(\theta_v = 0.031) = 1.9 \times 10^{50}$ erg), $E_p(0) = 340$ keV and $E_{\text{iso},\gamma}(0) = 1.6 \times 10^{54}$ erg are obtained. These values are similar to typical long GRBs. Then, the efficiency is $\eta_\gamma \approx 0.8$. If the narrow jet produces Episode 1, the estimated prompt emission efficiency η_γ is almost typical, however on-axis $E_p(0)$ is located at the highest end of the distribution for long GRBs. On the other hand, if the narrow jet emitted Episode 2, on-axis $E_p(0)$ is smaller though η_γ is somewhat higher. Episode 1 and 2 may be emitted from narrow and wide jets, respectively.

The prompt emission of GRB 190829A has lower $E_{\text{iso},\gamma}$ than the other VHE events. Hence, the outflow energy is expected to be too small for the SSC radiation to explain the VHE gamma-ray flux of GRB 190829A [3]. However, if GRB 190829A is viewed on-axis, then $E_{\text{iso},\gamma}(\theta_v = 0)$ and $E_p(\theta_v = 0)$ have typical values. Hence, the SSC emission from our large energy jet can explain the observed VHE gamma-ray flux (magenta solid line in Fig. 1).

Acknowledgments

We thank the organizers of the successful Gamma2022. This research was partially supported by JSPS KAKENHI Grant Nos. 22J20105 (YS), 20H01901 (KM), 20H05852 (KM), 19H01893 (YO), 21H04487 (YO) and 22H01251 (RY). SJT is supported by the Sumitomo Foundation for basic science research projects (210629), Research Foundation for Opto-Science and Technology, and Aoyama Gakuin University Research Institute. The work of KM is supported by the NSF Grant No. AST-1908689, No. AST-2108466 and No. AST-2108467. YO is supported by Leading Initiative for Excellent Young Researchers, MEXT, Japan.

References

- [1] Abdalla H., et al., *A very-high-energy component deep in the γ -ray burst afterglow*, *Nature*, **575** (2019) 464.
- [2] MAGIC Collaboration, *Observation of inverse Compton emission from a long γ -ray burst*, *Nature* **575** (2019) 455.
- [3] H.E.S.S. Collaboration, *Revealing x-ray and gamma ray temporal and spectral similarities in the GRB 190829A afterglow* *Science* **372** (2021) 1081.
- [4] O. Blanch, et al., *GRB 201216C: MAGIC detection in very high energy gamma rays*, *ATel* **14275** (2020).
- [5] V. Chand, et al., *Peculiar Prompt Emission and Afterglow in the H.E.S.S.-detected GRB 190829A*, *ApJ* **898** (2020) 42.
- [6] A.F. Valeev, et al., *GRB 190829A: 10.4m GTC spectroscopy*, *ATel* **25565** (2019).
- [7] Y.-D. Hu, et al., *10.4m GTC observations of the nearby VHE-detected GRB 190829A/SN 2019oyw*, *A&A* **646** (2021) A50.
- [8] L. Rhodes, et al., *Radio Afterglows of Very High Energy Gamma-Ray Bursts 190829A and 180720B* *MNRAS* **496** (2020) 3326.
- [9] O. S. Salafia, et al., *Multiwavelength View of the Close-by GRB 190829A Sheds Light on Gamma-Ray Burst Physics*, *ApJL* **931** (2021) L19.
- [10] S. Dichiara, et al., *The early afterglow of GRB 190829A*, *MNRAS* **512** (2022) 2337.
- [11] B. T. Zhang, et al., *External Inverse-Compton Emission from Low-Luminosity Gamma-Ray Bursts: Application to GRB 190829A*, *ApJ* **920** (2021) 55.
- [12] N. Fraija, et al., *On the origin of the multi-GeV photons from the closest burst with intermediate luminosity: GRB 190829A*, *ApJ* **918** (2021) 12.
- [13] L.-L. Zhang, et al., *Nearby SN-Associated GRB 190829A: Environment, Jet Structure, and VHE Gamma-Ray Afterglows*, *ApJ* **917** (2021) 95.

- [14] K. Ioka, T. Nakamura, *Peak Luminosity-Spectral Lag Relation Caused by the Viewing Angle of the Collimated Gamma-Ray Bursts*, *ApJL* **554** (2001) L163.
- [15] R. Yamazaki, K. Ioka, T. Nakamura, *X-Ray Flashes from Off-Axis Gamma-Ray Bursts*, *ApJL* **571** (2002) L31.
- [16] Y. Sato, et al., *Off-axis jet scenario for early afterglow emission of low-luminosity gamma-ray burst GRB 190829A*, *MNRAS* **504** (2021) 5647.
- [17] Y. Sato, et al., 2023, *Synchrotron Self-Compton Emission in The Two-Component Jet Model for Gamma-Ray Bursts*, *JHEAp* **37** (2023) 51.
- [18] Y. F. Huang, et al., *Overall Evolution of Jetted Gamma-Ray Burst Ejecta*, *ApJ* **543** (2000) 90.
- [19] R. Sari, A. A. Esin, *On the Synchrotron Self-Compton Emission from Relativistic Shocks and Its Implications for Gamma-Ray Burst Afterglows*, *ApJ* **548** (2001) 787.
- [20] E. Nakar, S. Ando, R. Sari, *Klein-Nishina Effects on Optically Thin Synchrotron and Synchrotron Self-Compton Spectrum*, *ApJ* **703** (2009) 675.
- [21] K. Murase, et al., *High-energy emission as a test of the prior emission model for gamma-ray burst afterglows*, *MNRAS* **402** (2010) L54.
- [22] K. Murase, et al., *On the Implications of Late Internal Dissipation for Shallow-decay Afterglow Emission and Associated High-energy Gamma-ray Signals*, *ApJ* **732** (2011) 77.
- [23] A. Franceschini, G. Rodighiero, M. Vaccari, *Extragalactic optical-infrared background radiation, its time evolution and the cosmic photon-photon opacity*, *A&A* **487** (2008) 837.
- [24] J. Granot, T. Piran, R. Sari, *Images and Spectra from the Interior of a Relativistic Fireball*, *ApJ* **513** (1999) 679.
- [25] P. A. Evans, et al., *An online repository of Swift/XRT light curves of γ -ray bursts*, *A&A* **469** (2007) 379.
- [26] P. A. Evans, et al., *Methods and results of an automatic analysis of a complete sample of Swift-XRT observations of GRBs*, *MNRAS* **397** (2009) 1177.
- [27] J. Granot, et al. *Off-Axis Afterglow Emission from Jetted Gamma-Ray Bursts*, *ApJL* **570** (2002) L61.
- [28] T. Q. Donaghy, *The Importance of Off-Jet Relativistic Kinematics in Gamma-Ray Burst Jet Models*, *ApJ* **645** (2006) 436.
- [29] C. Graziani, D. Q. Lamb, T. Q. Donaghy, *Gamma-Ray Burst Jet Profiles And Their Signatures*, *AIPC* **836** (2006) 117.
- [30] R. Yamazaki, K. Ioka, T. Nakamura, *Peak Energy-Isotropic Energy Relation in the Off-Axis Gamma-Ray Burst Model*, *ApJL* **606** (2006) L33.